Photo-Assisted Immobilized *Fenton* Degradation up to pH 8 of Azo Dye Orange II Mediated by Fe³⁺/*Nafion*/Glass Fibers

by **Mugunthu R. Dhananjeyan**[a]), **John Kiwi***[a]), **Peter Albers**[b]), and **Octav Enea**[c])

[a]) Department of Chemistry, Laboratory of Photonics and Interfaces, Swiss Federal Institute of Technology, CH-1015 Lausanne

[b]) *Degussa-Hüls AG*, Postfach 1345, 63403-Hanau/Main

[c]) UMR 6503 CNRS, University of F-Poitiers, 86022 Poitiers

Dedicated to Professor *André M. Braun* on the occasion of his 60th birthday

Fe³⁺ Ions have been immobilized into very thin *Nafion* films cast onto a glass-fiber mat immersed in an alcoholic solution of *Nafion* oligomers. This immobilized *Fenton* catalyst was used to abate/mineralize the azo dye Orange II, taken as a model organic compound. The abatement of Orange II on the Fe³⁺/*Nafion*/glass fibers was observed to proceed within the same time period as when *Nafion* alone was used to immobilize the Fe³⁺ ions during the photo-*Fenton* reaction. The amount of *Nafion* in the *Nafion* Fe³⁺/Nafion/glass fibers was *ca.* 15 times less per unit surface area compared to Fe³⁺-exchanged on conventional *Nafion* membranes used to immobilize Fe³⁺ ions. Orange II solutions under visible-light irradiation in the presence of H_2O_2 were mineralized up to pH 8 with a kinetics comparable to that found during the degradation runs at pH 3. Repetitive mineralization cycles mediated by the Fe³⁺/*Nafion*/glass fibers under visible light did not show any decrease in the activity of the immobilized catalysts. A reaction mechanism consistent with the experimental data is suggested. The morphology of the Fe³⁺/*Nafion*/glass fibers was characterized by scanning electron microscopy (SEM) showing thin *Nafion* films cast deposited on the glass fibers. Transmission-electron-microscopy (TEM) micrographs reveal Fe³⁺-oxy-hydroxide particles of 3–6 nm before and after repetitive Orange II photodegradation. X-Ray photoelectron spectroscopy (XPS) provided the evidence for the existence of Fe clusters on the topmost layer of the catalyst mainly as Fe^III. The improvements brought by the glass fibers are *a*) the use of low quantities of expensive *Nafion* supported on glass mats to achieve dye degradation rates comparable to *Nafion* alone and *b*) *Fenton*-mediated degradation of azo dyes at pH 8 without the costly initial acidification usually needed for this type of treatment.

1. Introduction. – During the last two decades, the degradation of aromatics, pesticides, herbicides, and other bio-recalcitrant compounds in industrial waste waters have been observed to proceed efficiently by oxidative radicals generated in the *Fenton* [1][2] and photo-assisted *Fenton* reactions [3–6]. However, the homogeneous photo-assisted *Fenton* generation of oxidative radicals in solution requires amounts of Fe³⁺ ions 10–20 times in excess of the 2–5 ppm levels allowed by the EEC [7] to be discharged directly into the environment. The removal of Fe ions of the system at the end of the treatment by precipitation and redissolution is costly in terms of chemicals and manpower, adding *ca.* 50% of the cost of *Fenton*-mediated degradation of industrial waters in the state of Delaware, USA [8]. The drawbacks of the homogeneous *Fenton* treatment of pollutants can be avoided by immobilizing Fe ions on a suitable substrate like *Nafion* [9] or on derivatized polymer films [10]. The materials to anchor Fe ions for the decomposition of H_2O_2 have to meet three criteria to catalyze in a stable fashion the degradation process: *a*) the substrate used has to be

resistant to the oxidizing radicals produced by the *Fenton* reagent in solution, *b*) the Fe ions on the substrate should not leach out into the solutions, and *c*) the degradation of the pollutant has to proceed at an acceptable kinetics. These criteria are met by *Nafion* perfluorinated membranes, which are chemically resistant to the highly oxidative OH· radicals and do not allow the leaching out of the Fe-exchanged on the sulfonic groups of the *Gierke* cages [11].

Azo dyes are an abundant class of synthetic colored organic compounds that comprise about half of the textile dyestuffs used today [12]. It is estimated that the release into the environment without proper treatment represents *ca.* 15% of total world production or 150 tons per day [13]. Orange II is a textile azo dye resistant to light degradation, the action of O_2, and common acids and bases. The stability of these dyes useful in textile applications makes them difficult to degrade. Moreover, Orange II does not undergo biological degradation in waste-water-treatment plants [14][15] and was taken as a model compound for azo-dye degradation. Azo dyes have been treated during the past 30 years by nondestructive technologies like filtration, granulated activated carbon (GAC), or by chemical coagulation with alumina [16]. The nondestructive methods transfer the contaminant from the waste water to the solid phase needing further processing or additional regeneration as in the case of GAC. Photochemical oxidation processes, which lead to the abatement of dyes involving OH· and HO_2· radicals generated at the surface of TiO_2 through photosensitized charge separations on the semiconductor surface, show a potential that is only now beginning to be explored. The destruction of azo dyes through photosensitized degradation on TiO_2 has been recently reported [17–19].

The objective of the present work is to investigate Orange II photodegradation on a new type of immobilized catalyst, the Fe^{3+}/*Nafion*/glass fibers and to report the details of the azo-dye degradation as a function of the common solution parameters. The morphology of Fe^{3+}/*Nafion*/glass fibers is characterized by up-to-date surface techniques. The main objectives of this study are *a*) to evaluate the performance of the low-cost Fe^{3+}/*Nafion*/glass fibers as compared with the Fe^{3+}/*Nafion* membranes previously reported [9] and *b*) to see whether the degradation of the model azo dye Orange II would proceed at pH > 4.8 to avoid the costly initial pH adjustment of many effluents to attain acidic conditions before applying the oxidative treatment Fe^{3+}/*Nafion*/glass fibers [9][20].

2. Results and Discussion. – 2.1. *Abatement of Orange II Solutions on Fe^{3+}/Nafion/Glass Fibers. Fig. 1* shows the color decrease (decoloration) of Orange II on Fe^{3+}/*Nafion*/glass fibers strips under visible-light irradiation in the presence of H_2O_2. Orange II was seen to decolor within 2 h, when the orange color of the aqueous solution disappeared. The color loss is due to the cleavage of the N=N bond of Orange II [15]. The decrease in the total organic carbon content (TOC) for Orange II solutions having different dye concentrations is shown in *Fig. 2*. The mineralization in the dark is seen to be < 10% for solutions of Orange II (0.20 mM) due to the decomposition of H_2O_2 by the Fe^{3+}/*Nafion*/glass fibers. Addition of H_2O_2 to Orange II (0.20 mM) did not lead to any observable mineralization in the absence of Fe^{3+}/*Nafion*/glass fibers. The mineralization of Orange II is seen to proceed under *Suntest* light irradiation for different concentrations of Orange II in *Fig. 2*. The steeper decline in the TOC
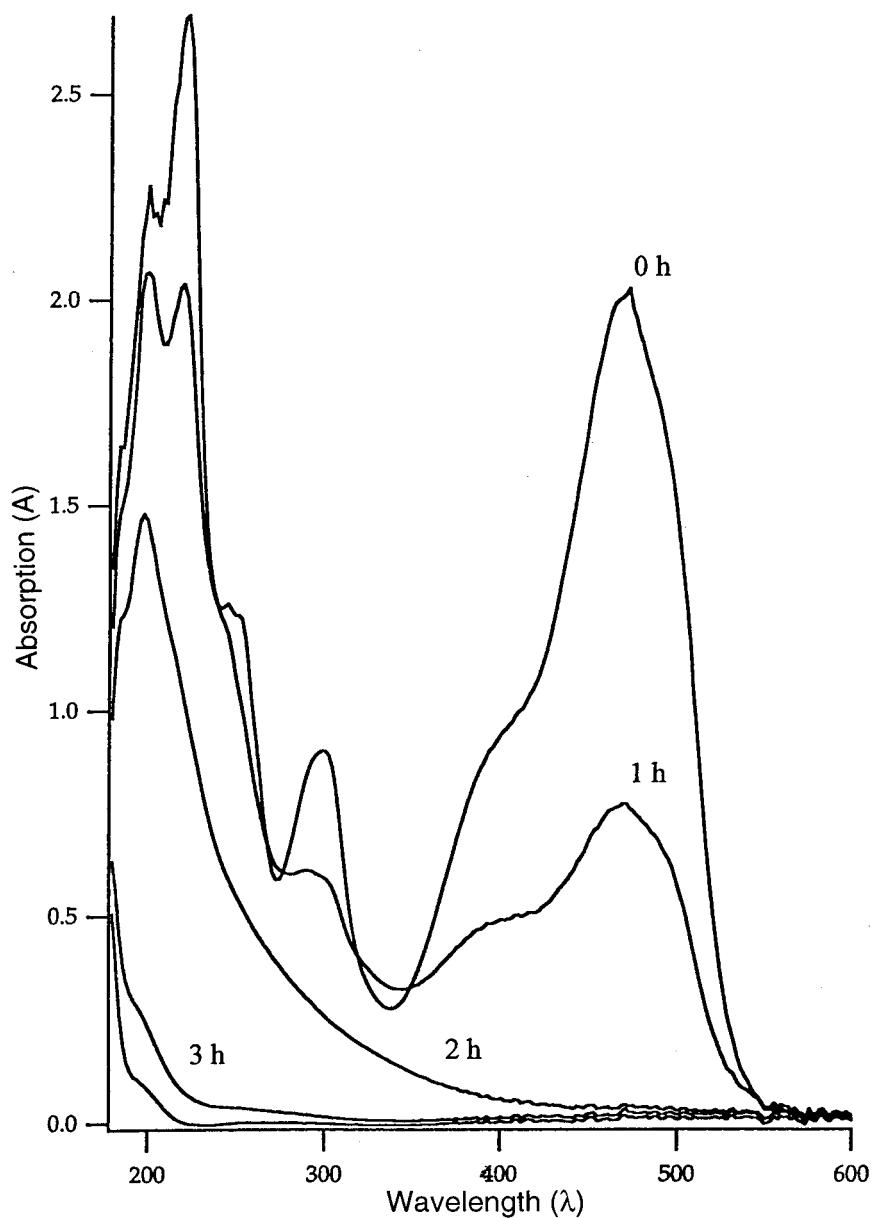
Fig. 1. *Decoloration of Orange II* (0.20 mM or TOC = 40 mg C/l) *on Fe³⁺/*Nafion*/glass fibers under* Suntest *light irradiation* (80 mW/cm²) *in the presence of H₂O₂* (10 mM) *at pH 3* (optical cell *d* = 0.5 cm)

observed at higher Orange II concentrations is due to the more favorable mass transfer taking place between the solution of Orange II and the Fe^{3+}/*Nafion*/glass fibers during reaction. The mass transfer between the solution and the Fe^{3+}/*Nafion*/glass fibers is
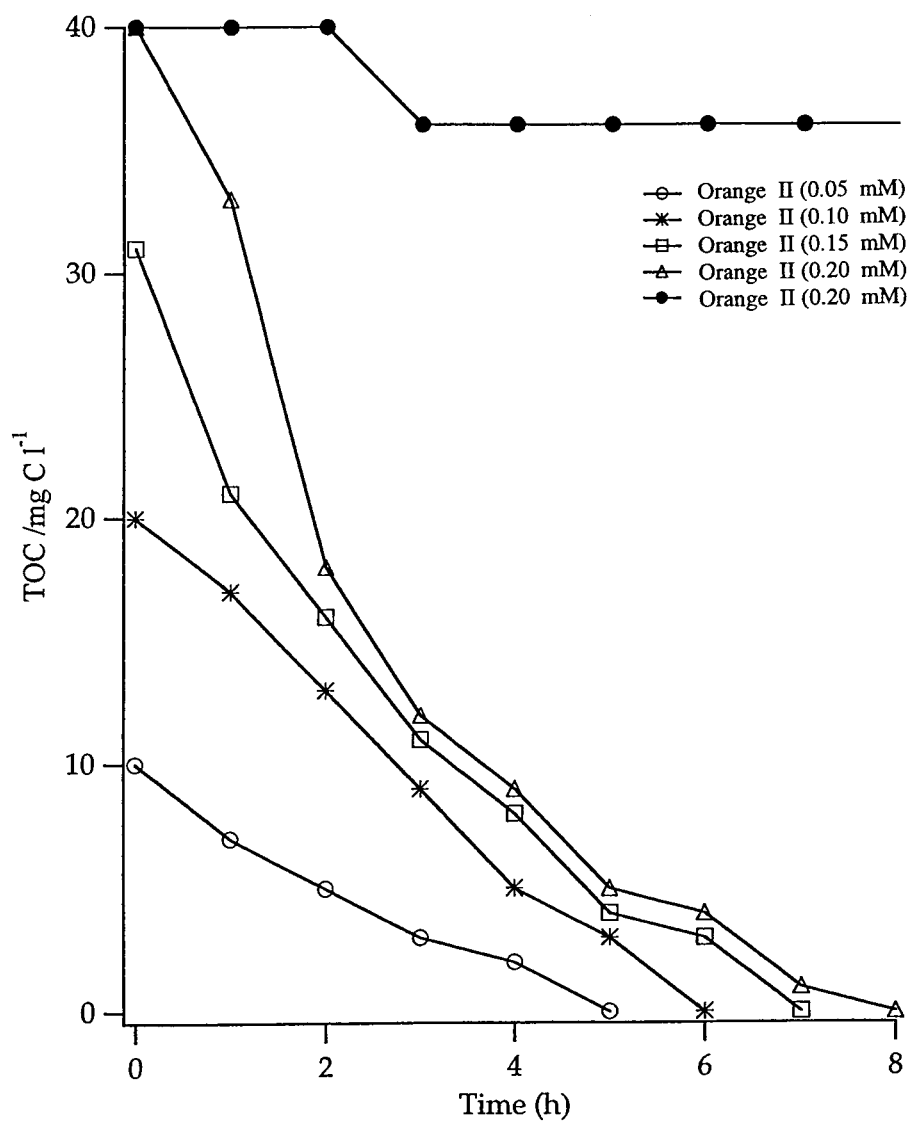
Fig. 2. *Mineralization of Orange II solutions of different concentrations on Fe^{3+}/Nafion/glass fibers in the dark and under* Suntest *light irradiation* (80 mW/cm^2) *in the presence of H_2O_2* (10 mM) *at pH 3.* Open points denote runs under light, and the filled points refer to the run in the dark.

driven by the difference in Orange II concentration existing between the bulk of the solution and the glass-mat interface. The diffusion length (x) of the oxidative-radical away from the glass mat can be estimated from the *Smoluchowski* diffusion relationship (*Eqn. 1*):

$$x^2 \approx D\tau \tag{1}$$

The rate of the reaction between the OH$^\cdot$ radical and Orange II has been recently reported to be close to 10^9 $M^{-1}s^{-1}$ [15][21]. At a concentration of Orange II (0.20 mM), the lifetime of the encounter pair is *ca.* 10^{-6} s. With $D \sim 5 \cdot 10^{-6}$ cm^2/s, a value for the diffusion length (x) of *ca.* 50 nm (*Eqn. 1*) is found for the OH$^\cdot$ radical. In the case of the HO$_2^\cdot$ radical, the value of the reaction rate of HO$_2^\cdot$ with Orange II is *ca.* 10^6 $M^{-1}s^{-1}$. From this, a value of *ca.* 310 nm can be estimated for the diffusion length of HO$_2^\cdot$ radical away from the Fe^{3+}/*Nafion*/glass.

The effect of the H$_2$O$_2$ concentration on the Orange II degradation was seen experimentally to be important. Upon addition of H$_2$O$_2$ (2.5 mM), slow and incomplete degradation was observed, which became faster when the oxidant was added at a higher concentration (12.5 mM). Beyond the later concentration and up to 30 mM H$_2$O$_2$, the photodegradation slows down, since the propagation step would be hindered by excess H$_2$O$_2$ scavenging the OH$^\cdot$ radicals available in solution (*Eqn. 2*)

$$H_2O_2 + OH^\cdot \;\rightarrow\; H_2O + HO_2^\cdot \qquad\qquad (2)$$
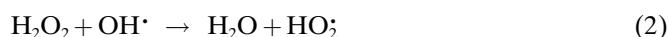
2.2. *The Variation of pH during Orange II Mineralization on Fe^{3+}/Nafion/Glass Fibers under Light Irradiation.* *Fig. 3* presents the results of the degradation of Orange II in the presence of H$_2$O$_2$ under *Suntest* light irradiation at different pH values. It is seen that *a*) in a wide pH range the mineralization of the azo dye takes place, and *b*) the photodegradation at pH values 5.5 and 8.0 mineralized *ca.* 86% of the initial Orange II. The later experimental results is a considerable improvement over the results obtained previously with the Fe^{3+}/*Nafion* systems [9]. In effect, mineralization of Orange II under *Suntest* irradiation on Fe^{3+}/*Nafion* was observed to proceed up to pH 4.8 attaining *ca.* 50% mineralization of the Orange II. At pH 2.8, complete mineralization was observed, which declined in efficiency towards higher pH values. The decoloration of Orange II on the Fe^{3+}/*Nafion* membrane under *Suntest* irradiation proceeded only up to pH 4.8, while, on Fe^{3+}/*Nafion*/glass fibers, the observed decoloration kinetics (not shown) was the same in the pH range 2.8–9.0. Acidification is needed to treat many effluents from the textile industry, which have an inherent pH value of 7–8. To carry out *Fenton* or photo-assisted *Fenton* homogeneously, the pH values have to be lowered < 4 as reported in several studies [2][6][5][14][20]. Immobilized *Fenton* systems as presented in this study avoid the costly initial acidification, which is sometimes more costly than the energy and oxidant used in the *Fenton*-mediated degradation [2][8][14]. The final pH values observed after *ca.* 9 h reaction (*Fig. 3*) were: pH 3.5 for an initial pH 3.0; pH 4.0 for an initial pH 5.5, and finally pH 4.5 for an initial pH 8.0. The pH drop during the reaction when starting with pH 5.5 and 8.0 is due to two factors: *a*) mineralization of Orange II produces HSO$_4^-$ and predominantly NH$_4^+$ [3][6][22][23]. Both contribute to acidify the solution, and *b*) intermediate Fe complexes consisting of Fe chelates are formed, leading to carboxylic acids during the degradation of Orange II. Oxalic, formic, and acetic acid, and smaller concentrations of other acids have been reported [23]. The pK_a of these acids correspond to the pH found in solution at the end of the degradation reported in *Fig. 3*. The degradation of Orange II shown in *Figs. 2–6* involving the formation of Fe-organic complexes is noted in *Eqn. 3*

$$[RCOO-Fe]^{2+} + h\nu \;\rightarrow\; [R^\cdot] + CO_2 + Fe^{2+} \qquad\qquad (3)$$

where the LMCT complex is the precursor step responsible for the TOC decrease reported in *Figs. 2–4*. The process given in *Eqn. 3* would proceed concomitantly to the radical reaction

$$RH + HO^{\bullet}\,(HO_2^{\bullet}) \;\rightarrow\; [R^{\bullet}] + RHOH \text{ or } H_2O \tag{4}$$

Evidence for the intervention of mass transfer processes involving oxidative radicals during the degradation of Orange II mediated by Fe^{3+}/*Nafion*/glass fibers are seen by inspection of *Fig. 2* and discussed already in *Sect. 2.1*.
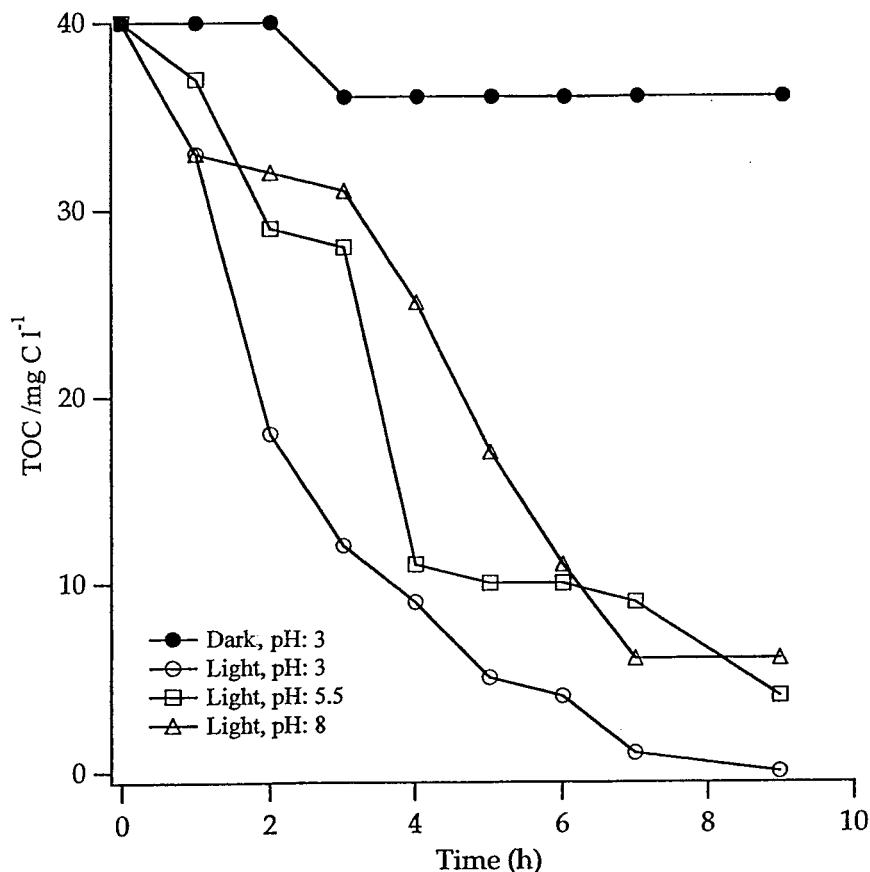

Fig. 3. *Mineralization of Orange II* (0.20 mM) *in the dark* (filled points) *and under* Suntest *light irradiation* (open points) *on Fe³⁺/*Nafion/*glass fibers at three different initial pH values in the presence of H₂O₂* (10 mM)
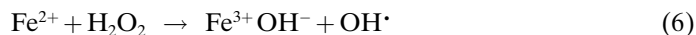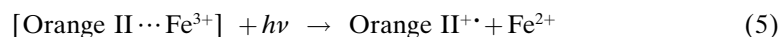
The degradation of Orange II under the same conditions on *Nafion* membranes was reported by our group some time ago [9] and proceeds only up to pH 4.8. In the case of Fe^{3+}/*Nafion*/glass fibers, *Harmer et al.* [24] have shown that acid groups of the *Nafion* are more accessible in *Nafion*-silica composites and display a greater chemical activity. The increased accessibility of these sulfonic groups leads to an improved ion-exchange

capacity mainly at the interface between the two materials. Additional or different Fe clusters may form on the *Nafion*/silica-matrix interface compared to the exchange of Fe ions on with the sulfonic groups of *Nafion* alone.
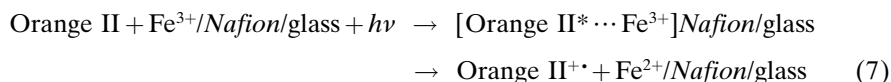
2.3. *Effect of Light Intensity and Catalytic Nature of the Mineralization of Orange II on Fe^{3+}/*Nafion*/Glass Fibers*. The photodegradation efficiency is seen to increase with the applied light intensity in the *Suntest* cavity (see *Exper. Part*), suggesting a dye-sensitized process. Additional comments to this are stated below in *Sect. 2.4* and *Fig. 5*.

Fig. 4 presents the catalytic nature of the decoloration of Orange II under *Suntest* irradiation on Fe^{3+}/*Nafion*/glass fibers in the presence of H_2O_2. At the end of each degradation cycle, suitable amounts of Orange II and H_2O_2 were added to the original solution as selected for the photocatalysis. The results in *Fig. 4* confirm the photo-catalytic nature of Orange II degradation. No measurable amounts of Fe^{3+} ions were found by application of the thiocyanate test. The absence of Fe^{2+} ions was demonstrated by complexation with phenanthroline.

2.4. *Mechanistic Aspects of the Interaction of Orange II and Fe^{3+}/*Nafion*/Glass Fibers under Visible-Light Irradiation*. It has been previously reported that Fe ions during homogeneous *Fenton* treatment form complexes with a variety of phenols, quinones, and other organic compounds [2][4][6][24]. In the case of Orange II, flash-photolysis studies of these Fe complexes were shown to lead to Fe^{2+}, which subsequently regenerated Fe^{3+} under light irradiation (*Eqns. 5* and *6*)

$$[\text{Orange II} \cdots \text{Fe}^{3+}] + h\nu \rightarrow \text{Orange II}^{+\cdot} + \text{Fe}^{2+} \tag{5}$$

$$\text{Fe}^{2+} + \text{H}_2\text{O}_2 \rightarrow \text{Fe}^{3+}\text{OH}^- + \text{OH}^{\cdot} \tag{6}$$

Photosensitization by Orange II of Fe^{3+} solutions has been reported recently by flash photolysis leading to charge-transfer quenching by the excited Orange II* [22][25]. The initial step of Orange II acting as the sensitizer of Fe^{3+}/*Nafion*/glass fibers was suggested as given in *Eqn. 7*

$$\text{Orange II} + \text{Fe}^{3+}/Nafion/\text{glass} + h\nu \rightarrow [\text{Orange II}^* \cdots \text{Fe}^{3+}]Nafion/\text{glass}$$
$$\rightarrow \text{Orange II}^{+\cdot} + \text{Fe}^{2+}/Nafion/\text{glass} \tag{7}$$

This is consistent with the results reported in *Figs. 2* and *3* that the mineralization of Orange II in the dark is very slow compared to the one taking place under light irradiation due to the slow conversion kinetics of Fe^{3+} to Fe^{2+}.

Fig. 5 shows the degradation scheme of Orange II under visible-light irradiation in the presence of H_2O_2. At the beginning of the reaction, the incident light is absorbed by the Orange II. The decoloration of Orange II is observed to proceed in *ca.* 2 h (*Fig. 1*). This is four times faster than the mineralization observed for a solution of Orange II (0.20 mM) as shown in *Fig. 2*. Therefore, after the dye-sensitized degradation process shown in *Eqn. 7*, the long-lived transparent intermediates are degraded further by the Fe^{3+}/*Nafion*/glass fibers under light. The Fe^{3+}/*Nafion*/glass fibers show a layer of Fe-oxy-hydroxide red-brown particles that are able to absorb light in the visible region. The red-brown color of the glass mat is observed to fade slightly after repeated use (*Fig. 4*). The reaction of Fe^{3+} with H_2O_2 ($k = 2 \cdot 10^{-3}$ M^{-1}s^{-1}) is much slower than the
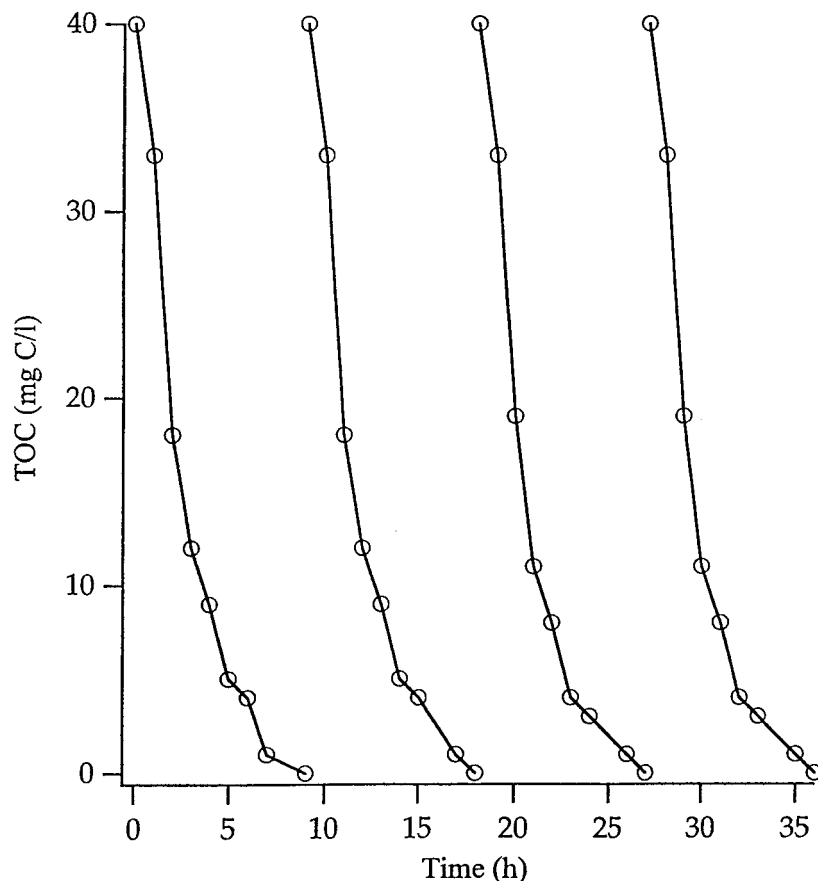
Fig. 4. *Repetitive photocatalytic mineralization of Orange II* (0.20 mM) *on Fe³⁺/*Nafion*/glass fibers under* Suntest *light irradiation in the presence of H₂O₂* (10 mM) *at an initial pH 3*

reaction of Fe^{2+} with H_2O_2 ($k = 60$ M^{-1}s^{-1}). This accounts for the small amount of Fe^{II} formed in the steady state in homogeneous reactions and also on the surface of the iron-loaded glass mats, since the reaction with H_2O_2 is very fast. To account for the fading observed, we have carried out XPS and FTIR of the iron-loaded glass mats before and after reaction. We have not been able to ascribe with precision Fe peaks to Fe^{III} and Fe^{II} before and after reaction. We observe three peaks related to Fe-oxy-hydroxy-species. It is not possible to separate the peaks to Fe^{II} and Fe^{III} in a clean way by the either technique used. The peaks observed by XPS do not correspond, after the *Shirley* correction [26], to the Fe^{II}/Fe^{III}-oxy-hydroxy-species, but to some intermediate valence state of Fe. This confirms a strong effect of the *Nafion* matrix on the Q-sized Fe. The fading of the initial color cannot at present be ascribed only to the growing in of Fe^{II} species. Polymeric forms of Fe ions or Fe ion-pair charge-transfer bands formed at the catalyst surface during the reaction may be responsible for the fading of color at the catalyst surface [4][5][27].
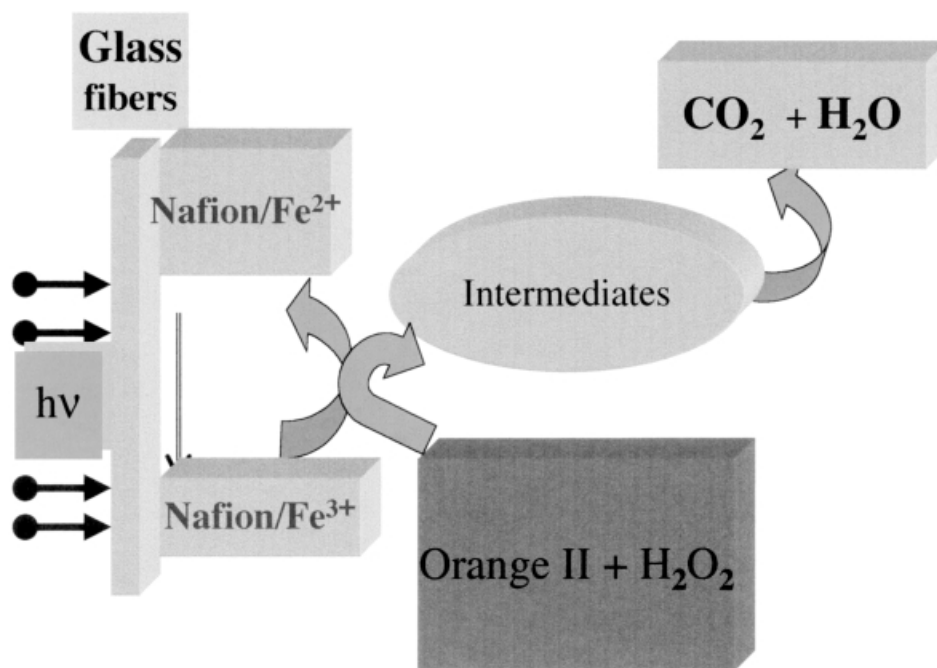
Fig. 5. *Mechanism of Orange II photocatalytic degradation mediated by Fe^{3+}/Nafion/glass fibers under Suntest visible-light irradiation*

2.5. *Physical Characterization of Fe^{3+}/Nafion/Glass Fibers Surface by BET, Electron Microscopy (TEM/SEM), and X-Ray Photoelectron Spectroscopy (XPS)*. The physical characterization of the immobilized Fe catalyst by four different and complementary methods is described below:

a) *Gas Adsorption Measurements*. A BET surface area < 1 m²/g was found for the glass mat before Fe^{3+}/*Nafion* loading. After iron loading, the surface area was seen to have decreased by *ca.* 10–15%.

b) *Scanning Electron Microscopy (SEM)*. SEM of the *Nafion* of the glass mat is shown in *Fig. 6*. The electron microscope (*JEOL-35 CF*) at 15 keV showed *Nafion* deposition mainly on the intersections of the glass fibers. The SEM also shows the flexible nature of the *Nafion* deposits on the supporting glass-mat fibers. The fibers of soda lime glass were seen to be 4–20 μ in diameter when taking into consideration SEM data over 100 single glass fibers. The stacking of glass fibers leading to the composite mat at the microscopic level did not follow any defined geometrical configuration.

c) *Transmission Electron Microscopy (TEM)*. The Fe particles were small and rather homogeneously dispersed. The dark spots in *Fig. 7* consist of Fe particles as analyzed by TEM combined with energy-dispersive X-ray microanalysis (STEM/EDX). The glass mats before use consisted of Fe particles with sizes in the range 3–6 nm. Glass mats after use presented highly dispersed Fe species with sizes in the range
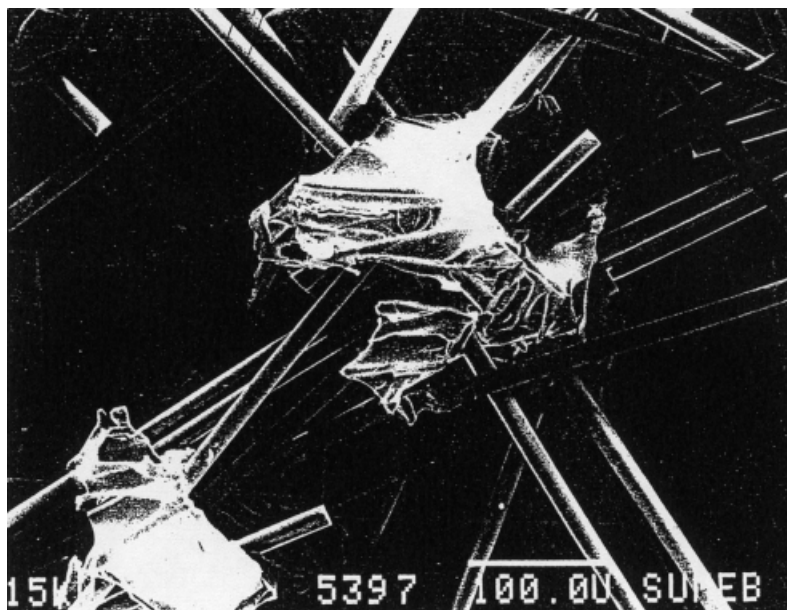
Fig. 6. *Scanning electron microscopy of the Fe^{3+}/*Nafion: *flexible nature of the* Nafion *deposit on the supporting glass fibers*

of 4–7 nm. The Fe clusters were found only on the *Nafion*-covered areas of the glass mats due to the method of preparation employed (see *Exper. Part*).

d) *X-Ray Photoelectron Spectroscopy (XPS)*. The XPS spectra were analyzed using a DS data-set (*Leybold*) after X-ray-satellite subtraction to smooth the signals by polynomial fit and background subtraction according to *Shirley* [26]. Electrostatic-charging effects were corrected by internal referencing to the C1s signal. A separate set of charge-compensation experiments were performed including changes of the electrostatic potential at the aperture of the XPS-electron analyzer by low-energy-electron dosing of the glow emission source. Fresh samples used had a sulfate content of 0.14% on the catalyst surface area. Sulfate was not found in the glass mats after use. N Compounds of the samples before use were detected as amines and ammonium-N in the amount of 1.35% of the catalyst surface area. After the Orange II degradation, no quantifiable N compounds were detected. Chloride ion found on the catalyst surface in the unused catalyst was decreased by a factor of three to *ca.* 0.05% of the surface total area after reaction. These observations point out to the efficient catalysis mediated by Fe^{3+}/*Nafion*/glass fibers, since only a very small amount of residues were detected at the catalyst surface. The values obtained took into account the relative sensitivity factors of the surface elements and had an accuracy of $\pm 5\%$.

The Fe detected in the topmost layer of the catalyst corresponds to Fe^{III} with a BE of 711.5 eV for a fresh catalyst and 712.1 eV after catalytic degradation of Orange II (see the *Table*). This indicates that a more oxidized form of Fe is present on the glass mat surface after the catalytic degradation of Orange II. For the quantitative
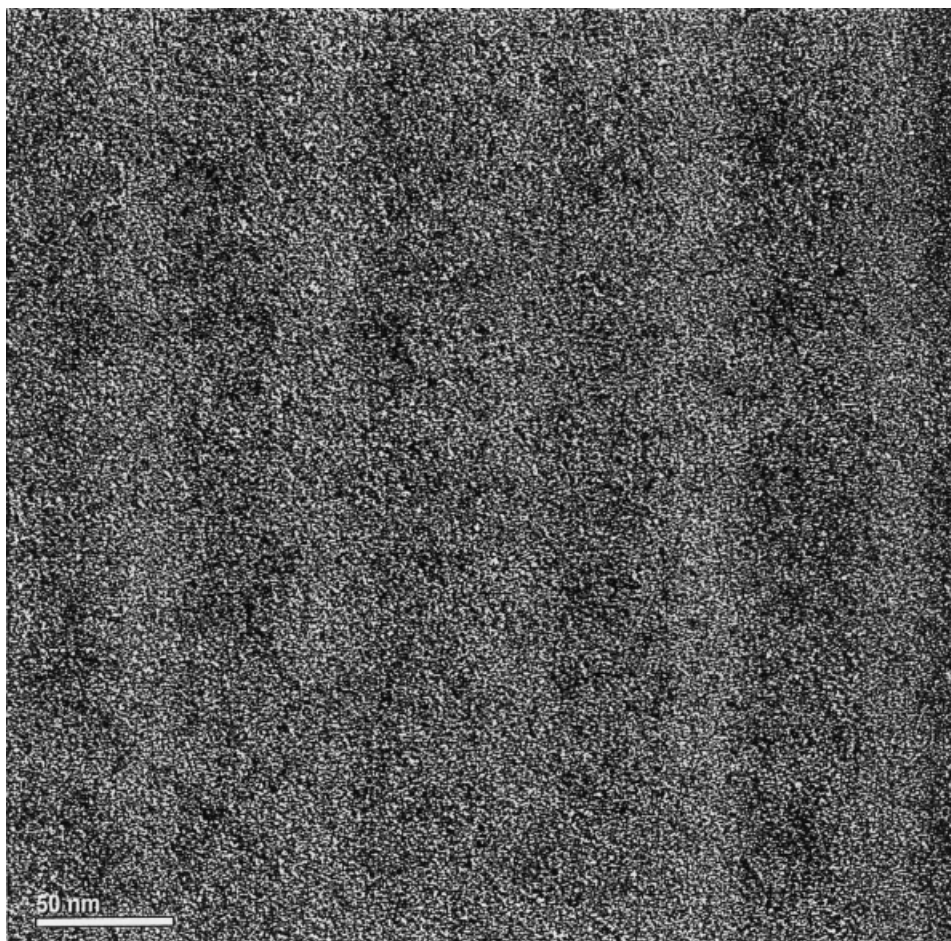
Fig. 7. *Transmission electron microscopy of Fe^{3+}/Nafion/glass fibers.* For other experimental details, see text.

computation of the XPS spectra, the signals were compared with signals reported for compounds with similar composition reported in the literature [28].

Experimental Part

Materials. Orange II, H_2O_2, HCl, $FeCl_3 \cdot 6 H_2O$, phenanthroline, KSCN, and i-PrOH were *Fluka* (*p.a.*) reagents and used as received. Triple-distilled H_2O was used in all experiments.

Preparation of the Fe^{3+}/Nafion/Glass Fibers. The glass mats were made up of soda-lime glass $4-20\,\mu$ in diameter having a BET area $< 1\,m^2/g$. The glass-fiber mat is treated [29] and impregnated with a *Nafion* perfluorinated ion-exchange resin in a mixture of alcohols and H_2O (45%) obtained from *Aldrich* (product No. 50,02-1). The membrane is then heated to eliminate the solvents and exchanged with an aq. soln. of $FeCl_3$ by a procedure reported in [9]. The *Nafion* membrane, used with an equivalent weight of *ca.* 1200, contains tetrafluorethylene and perfluorovinyl ether. It adsorbs large quantities of H_2O and other polar materials to swell the polymer. The hydrophilic sulfonate clusters of the *Nafion* maximize their interaction with the iron-hydrated polar species in solution [29][30], ensuring that the Fe ions are deposited only on the *Nafion* and not on the

Table. *Binding Energies* [eV] *of Surface Elements*

	Nafion droplets A	
	100 before use	101 after use
Na 1s	1072.6	1072.8
Fe 2p	711.5	712.1
F 1s	687.6	686.9
O 1s	532.1	532.7
N 1s	399.3	399.1
C 1s	284.5	284.5
Cl 2p	198.1	198.1
S 2p	169.1	–
Si 2p	102.6	103.1
Al 2p	74.2	74.5

silica glass mat. The deposition of Fe oxy-hydroxide of red-brown color was not evenly distributed on the glass mat, and, therefore, the amounts of Fe clusters per unit area were not the same from different preparations. But the overall activity of the 48 cm^2 Fe^{3+}/*Nafion*/glass fibers strips used in degradation experiment was reproducible to $\pm 10\%$. Fe^{3+}/*Nafion*/glass fibers strips were kept in aq. soln. throughout this work to attain better reproducibility during the degradation runs to avoid changes with time of the Fe-oxy-hydroxide deposited on the glass-mat surfaces.

Photoreactor and Irradiation Procedures. The irradiation vessels used were 60-ml cylindrical *Pyrex* flasks (cutoff λ 290 nm) each containing 40 ml of reagent soln. The Fe^{3+}/*Nafion*/glass fibers strips of 48 cm^2 were placed immediately behind the wall of the reaction vessel. Irradiation of the Orange II solns. in the vessels was carried out inside the cavity of a *Hanau Suntest* air cooled at *ca.* 46°. The *Suntest* lamp had a wavelength (λ) distribution with *ca.* 7% of the emitted photons between 290 and 400 nm. The profile of the photons emitted by the *Suntest* between λ 400 nm up to 800 nm followed closely the solar spectrum. The *Suntest* solar simulator had an intensity of 80 mW/cm^2 for λ between 290 and 800 nm. The intensity of the *Suntest* lamp could be tuned to different values. The radiant flux in mW/cm^2 was measured with a power-meter of the *LSI Corp.*, Yellow Springs, CO, USA.

Analysis of Irradiated Solns. Spectrophotometric analyses of the solns. before and after irradiation were carried out by means of a *Hewlett-Packard 8452* diode-array spectrophotometer. The total organic carbon (TOC) was monitored *via* a *Shimadzu 500* instrument equipped with an *ASI* automatic sample injector. The peroxide concentrations were assessed by *Merckoquant* paper at levels between 0.5 and 25 mg/l of H$_2$O$_2$.

Transmission Electron Microscopy (TEM) and Scanning Electron Microscopy (SCE). A field-emission TEM *JEOL 2010F* (300 kV, 2 Å point resolution) equipped for energy-dispersive X-ray microanalysis (EDX) was used. The sample fabric was coated with epoxy and cut with a microtome to a thin layer at a 90° angle and deposited onto a C foil. Energy-dispersive X-ray-analysis (EDAX) was used to identify the Fe clusters on the support. SCE was carried out with a *Philips/300S* instrument.

Gas-Adsorption Studies. Physisorption was carried out *via* a *Sorptomatic 1990 Micropore* unit. A precision of 2% was attained in the reproducibility in the adsorption isotherms. The experiments were performed at liq. N$_2$ boiling temp. (77 K). The surface area was evaluated in each case with the help of a computerized *19190 Micropore* system.

The X-Ray Photoelectron Spectroscopy (XPS). Experiments were performed with a *Leybold-Heraeus* instrument (*LHS 12*) and MgK_α radiation at a power of 200 W. Binding energies of the peaks were referenced to the Au 4 f 7/2 energy level of 84 eV. The spectra were analyzed in a *DS-100* data set (*Leybold*) after X-ray satellite subtraction and smoothing by polynomial fit. The quant. evaluation of the background correction was based on the standard *Shirley* [26] treatment. The relative sensitive factors used were: Fe2p: 2.91, O1s: 0.78, C1s: 0.34, and S2p: 0.84. Electrostatic charging effects were referenced by calibration to the C1s signal. Charge compensation measurements involved changing the electrostatic potential at the entrance slit of the XPS electron analyzer.

REFERENCES

[1] C. Walling, *J. Am. Chem. Soc*. **1975**, *8*, 125.

[2] R. Bauer, G. Waldner, H. Fallmann, T. Kreutzler, S. Malato, P. Maletzky, *Catal. Today* **1999**, *53*, 131.

[3] G. Rupert, R. Bauer, G. Heisler, *J. Photochem. Photobiol. A, Chem*. **1993**, *73*, 75.

[4] S. Bossmann, E. Oliveiros, S. Göb, S. Siegwart, A. M. Braun, *J. Phys. Chem. A* **1996**, *102*, 5542.

[5] J. Kiwi, A. Lopez, V. Nadtochenko, *Environ. Sci. Technol.* **2000**, *34*, 2162.

[6] J. Pignatello, D. Liu, P. Huston, *Environ. Sci. Technol*. **1999**, *33*, 1832.

[7] European Economic Community List of Council Directives 76/4647, Brussels 1992.

[8] C. P. Huang, in 'Remediation of the Aquatic and Atmospheric Environment by Advanced Oxidation', Ed. Po-Lock Yue, Hong-Kong, China, World Scientific Pub. 2000.

[9] J. Fernandez, J. Bandara, A. Lopez, Ph. Buffat, J. Kiwi, *Langmuir* **1999**, *15*, 185.

[10] M. Dhananjeyan, J. Kiwi, R. Thampi, *Chem. Commun*. **2000**, 1443.

[11] T. Gierke, G. Munn, F. Wilson, *J. Polym. Sci., Polym. Phys. Ed*. **1981**, *19*, 1687.

[12] H. Zollinger, 'Color Chemistry, Properties and Applications of Organic Dyes and Pigments', VCH, Weinheim, 1987.

[13] C. Maynard, 'Handbook of Industrial Chemistry', Van Nostrand Publ. New York. 1983.

[14] E. Balanosky, F. Herrera, A. Lopez, J. Kiwi, *Water Res*. **2000**, *34*, 582.

[15] V. Nadtochenko, J. Kiwi, *J. Chem. Soc., Faraday Trans*. **1997**, *93*, 2373.

[16] T. Crowe, C. O'Melia, L. Little, *Am. Dyestuff* **1978**, 52.

[17] D. Vinodgopal, D. Wynkoop, P. V. Kamat, *Environ. Sci. Technol*. **1996**, *30*, 1660.

[18] L. Lucarelli, V. Nadtochemko, J. Kiwi, *Langmuir* **2000**, *16*, 1102.

[19] C. Galindo, P. Jaques, A. Kalt, *J. Adv. Oxid. Technol's* **1999**, *4*, 400.

[20] E. Balanosky, J. Fernandez, J. Kiwi, A. Lopez, *Water Sci. Technol*. **1999**, *40*, 417.

[21] J. Bandara, J. Mielczarski, J. Kiwi, *Langmuir* **1999**, *15*, 7680.

[22] V. Nadtochenko, J. Kiwi, *Inorg. Chem* **1998**, *37*, 5223.

[23] J. Bandara, J. Kiwi, *New J. Chem*. **1999**, *23*, 717.

[24] A. Harmer, E. Farneth, Q. Sun, *J. Am. Chem. Soc*. **1996**, *118*, 7708.

[25] C. Morrison, J. Bandara, J. Kiwi, *J. Adv. Oxid. Technol's* **1996**, *1*, 160.

[26] A, Shirley, *Phys. Rev*. **1979**, *B5*, 4709.

[27] J. Kiwi, A. Denisov, V. Nadtochenko, *J. Phys. Chem. B* **1999**, *103*, 9141.

[28] Report DMA (A) National Physics Laboratory, Teddington, UK, 1997.

[29] European Patent Application (pending), EPFL, Lausanne, Switzerland, 2001.

[30] *Aldrich*, 'Technical Information Bulletin No. AL-163', Aldrich Chem. Co. 1992.